Dublin Institute of Technology
ARROW@DIT

Articles

School of Electronic and Communications Engineering

2011-01-01

A High Sensitivity, Evanescent Feld Refractometric Sensor Based on Tapered Multimode Fiber Interference

Pengfei Wang
Dublin Institute of Technology, pengfei.wang@dit.ie

Gilberto Brambilla
University of Southampton

Ming Ding
University of Southampton

Qiang Wu
Dublin Institute of Technology, qiang.wu@dit.ie

Gerald Farrell
Dublin Institute of Technology, gerald.farrell@dit.ie

Follow this and additional works at: http://arrow.dit.ie/engscheceart

Part of the Electromagnetics and photonics Commons

Recommended Citation

Wang, P., Brambilla, G., Ding, M., Semenova, Y., Wu, Q., Farrell, G.:A High Sensitivity, Evanescent Feld Refractometric Sensor Based on Tapered Multimode Fiber Interference. Optics Letters, Vol. 36, 12, 2011, pp.2233-2235.

This Article is brought to you for free and open access by the School of Electronic and Communications Engineering at ARROW@DIT. It has been accepted for inclusion in Articles by an authorized administrator of ARROW@DIT. For more information, please contact yvonne.desmond@dit.ie, arrow.admin@dit.ie.

This work is licensed under a Creative Commons Attribution-Noncommercial-Share Alike 3.0 License

High-sensitivity, evanescent field refractometric sensor based on a tapered, multimode fiber interference

Pengfei Wang,[1,2,*] Gilberto Brambilla,[1] Ming Ding,[1] Yuliya Semenova,[2] Qiang Wu,[2] and Gerald Farrell[2]

[1]*Optoelectronics Research Centre, University of Southampton, Southampton SO17 1BJ, UK*

[2]*Photonics Research Center, School of Electronic and Communications Engineering, Dublin Institute of Technology, Kevin Street, Dublin 8, Ireland*

**Corresponding author: pw3y09@orc.soton.ac.uk*

Received April 5, 2011; revised May 13, 2011; accepted May 17, 2011; posted May 18, 2011 (Doc. ID 145440); published June 7, 2011

We propose and experimentally demonstrate an enhanced evanescent field fiber refractometer based on a tapered multimode fiber sandwiched between two single-mode fibers. Experiments show that this fiber sensor offers ultra-high sensitivity [better than 1900 nm/RIU at a refractive index (RI) of 1.44] for RI measurements within the range of 1.33–1.44, in agreement with the theoretical predictions. This is the highest value reported to date (to our knowledge) in the literature. © 2011 Optical Society of America

OCIS codes: 060.2310, 060.2370, 060.3510.

Optical fiber refractometers have been widely investigated for chemical and biotechnological applications due to a range of unique advantages, such as low cost, compact size, high resolution, multiplexing ability and usage in harsh environments, immunity to electromagnetic interference, and the potential for remote operation [1–8]. To date, a number of fiber refractometers have been developed using a fiber Bragg grating [1], macrobend single-mode fiber (SMF) [2], surface plasmon resonance [3], a Fabry–Perot interferometer [4], a microsphere resonator [5], an optical ring resonator [6], and a microfiber coil resonator [7]. As an alternative to these existing fiber refractometers, a single-mode–multimode–single-mode (SMS) fiber refractometer utilizing multimode interference in the multimode fiber (MMF) core section has been recently proposed [8]: this allowed for the measurement of the refractive index (RI) with a resolution of 5.4×10^{-5} refractive index units (RIUs).

In this Letter, we report the experimental demonstration of a novel, high-sensitivity refractometric sensor based on multimodal interference in single-mode–tapered multimode–single-mode fiber structures (STMS) capable of improving the resolution by at least 1 order of magnitude.

For RI sensing, a large overlap between the propagating mode and the surrounding fluid needs to take place; thus, the MMF cladding in the SMS structure needs to be removed. Experimentally, the fiber cladding can be etched using hydrofluoric acid, but this increases the fabrication difficulty and the induced surface roughness may lead to a significant discrepancy between experimental results and theoretical design [2]. Alternatively, a tapered structure can replace the chemical etching process; because light guided in a tapered fiber has a significant fraction of power propagating in the evanescent wave, the effective index of the guided mode is affected by the external medium RI. It is well known that the fraction of power in the evanescent wave, thus its sensitivity to environmental changes, increases at small taper diameters. Because untapered MMFs have a large core diameter and a large NA, the power in the evanescent field is very small, and strong tapering is needed to increase it.

The schematic configuration of STMS used in these experiments is shown in Fig. 1: the fiber structure under consideration consists of an input SMF, a tapered MMF section, and an output SMF. Light propagation in the MMF section has been simulated employing a beam propagation technique: a wide-angle beam propagation method (WABPM) in cylindrical coordinates using the Padé (3, 3) approximate operator and perfectly matched layer (PML) boundary conditions [9]. The calculated amplitudes of the optical fields of both untapered and tapered SMS fiber structures are presented in Figs. 2(a)–2(c), respectively. Figure 2(a) shows the expected optical field for an untapered MMF section for reference, while Figs. 2(b) and 2(c) show that strong mode interference occurs within the tapered MMF section due to the focusing effects of the left tapered transition region. Within the tapered MMF section, the excited modes of LP_{0m} in the MMF core will be partly coupled to the high-order cladding modes at the beginning of the fiber taper region, and this increases the fraction of power in the evanescent wave within the region of the MMF cladding.

The SMS sample was manufactured from a 42 mm long Thorlabs AFS105/125Y step-index MMF, which was stripped, cleaved, and then spliced between two standard SMFs. As shown in Fig. 3(a), a CO_2 laser (Synrad, Model 48-2KWL, with maximum power of 30 W at a wavelength of 10.6 μm) was employed to fabricate the tapered fiber. A ZnSe cylindrical lens with focal length of $254 \pm 0.5\%$ mm focused the CO_2 laser beam to ~150 μm. Beam movement was achieved using gold-coated mirrors on a motorized translation stage (Aerotech ABL1500). A LabView program controlled the shutter opening and, therefore, the laser exposure time. Two 3D translation stages were used to adjust the heating position within the MMF section, while two weights (3 g each) were used to apply a constant tension to the SMF ends of the fiber

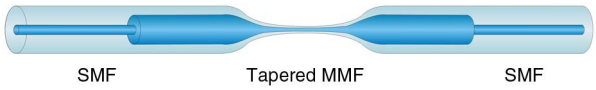

Fig. 1. (Color online) Schematic configuration of the STMS structure.

 © 2011 Optical Society of America

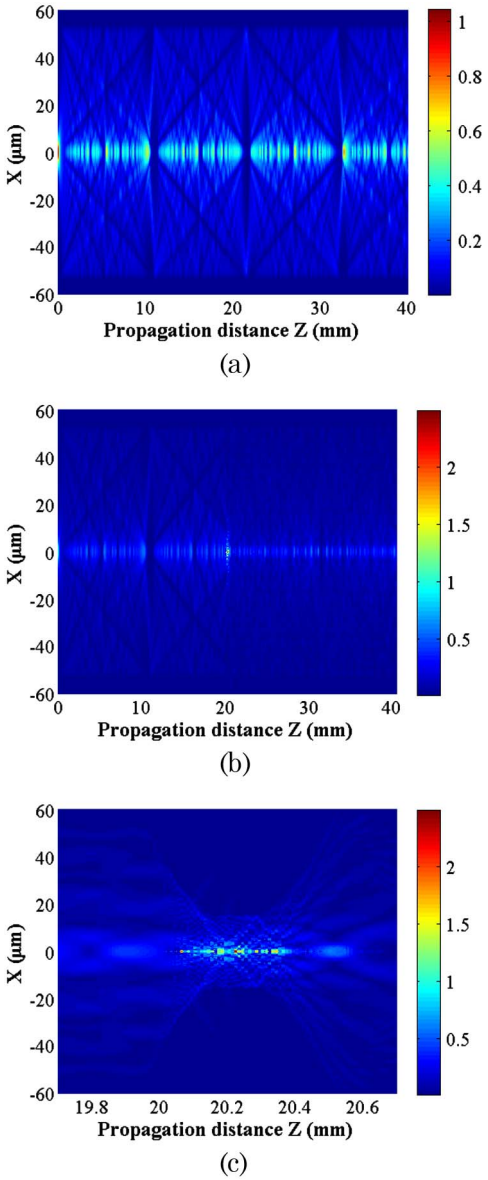

Fig. 2. (Color online) Calculated amplitude of optical fields using a WABPM for (a) untapered and (b) tapered step-index MMF sandwiched between two standard SMFs and (c) optical field image for tapered region within the MMF section [magnification of (b)]. The length of the untapered MMF is 40 mm; the diameter and the length of the uniform waist are 30 μm and 150 μm, respectively; and the operating wavelength is 1550 nm.

structure. The middle of the MMF was exposed to the CO_2 laser beam with an output power of 15 W and tapering occurred because of the tension applied to the SMFs. The resulting taper is shown in Fig. 3(b): the waist diameter and total taper length were $D \sim 30\,\mu$m and $L \sim 675\,\mu$m, respectively. The transmission spectra of the tapered SMS were recorded during fabrication using a broadband LED source and a high-resolution (20 pm) optical spectrum analyzer (Yokogawa AQ6370).

Figure 4 presents the calculated and measured transmission spectra of the SMS fiber structures before and after the tapering process. The measured results show a good agreement with theoretical predictions. The discrepancy between the calculated and measured results

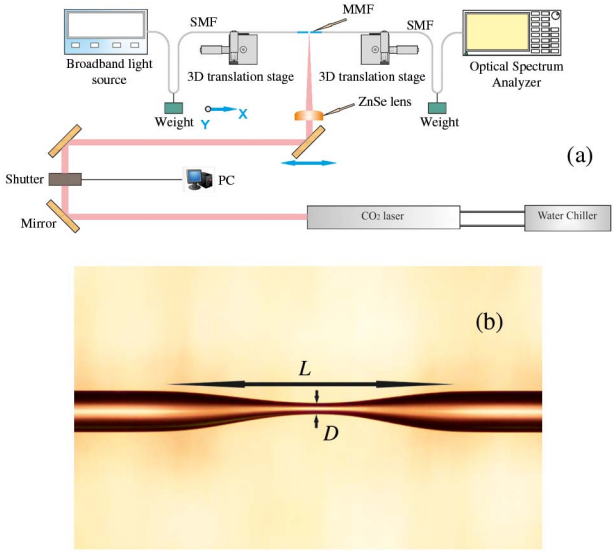

Fig. 3. (Color online) (a) Experimental setup for fiber tapering. (b) Microscope image of tapered MMF.

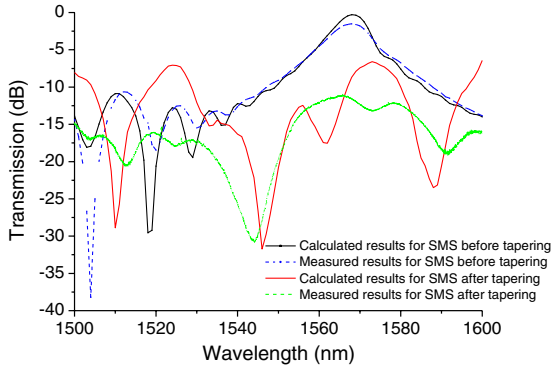

Fig. 4. (Color online) Calculated and measured spectral responses of untapered and tapered SMS over a wavelength range of 1500–1600 nm.

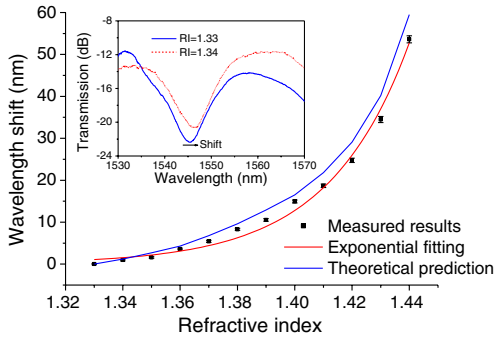

Fig. 5. (Color online) Calculated and measured peak wavelength shifts as a function of the RI. Inset, measured spectral responses of tapered SMS with surrounding RI liquids of 1.33 and 1.34, respectively.

could be due to both the deformed shape of the fabricated taper and the approximations made in the calculation [transmission for a tapered SMS includes some approximations, such as the Padé (3, 3) approximate operator].

The RI sensing measurement was performed at room temperature (~25 °C) with a series of RI liquids

Table 1. Resolution for Evanescent Field Fiber Refractometric Sensors (Assuming the Minimum Resolution of the Wavelength Peak Shift Is 10 pm)

No.	Type of Sensor	Resolution (RIU)	Ref.	Notes
1	SMF taper Michelson interferometer	3.45×10^{-4}	[12]	Terminated by ~500 nm thick gold coating
2	Optical liquid ring resonator, coated glass capillary, and fiber taper	$\sim 1 \times 10^{-4}$	[13]	Wall thickness 0
3	Notched microfiber probe	$\sim 9.09 \times 10^{-5}$	[14]	3.5 μm micronotch cavity
4	Tapered graded index MMF	$\sim 3 \times 10^{-5}$	[15]	MMF diameter ~60 μm
5	Optical fiber nanowire sensor	$\sim 1 \times 10^{-5}$	[16]	Optical fiber microcoil radius ~300 nm (theoretical results)
6	Optical fiber microcoil grating	$\sim 8.33 \times 10^{-6}$	[17]	Optical fiber microcoil radius ~200 nm (theoretical results)
7	Etched SMS fiber	$\sim 5.51 \times 10^{-6}$	[18]	MMF diameter ~80 μm
8	Tapered SMS fiber	$\sim 5.23 \times 10^{-6}$	This work	

(1.33–1.44 with an interval of 0.01, RI error $\pm$ 0.0002). The RI liquids were placed around the taper using a dropper. Light from a broadband light source 1450–1650 nm was launched into the tapered SMS, and the transmitted light was collected by the optical spectrum analyzer. The simulated and experimental wavelength shifts at the maximal transmission peak are plotted in Fig. 5 as a function of the RI. As expected from simulations (blue solid curve), the curve follows an essentially exponential distribution with an average sensitivity of 487 nm/RIU over an RI range of 1.33–1.44. The experimental results match the theoretical simulations reasonably well. A maximum sensitivity of 1913 nm/RIU is achieved for RI ~ 1.44, resulting in a resolvable index change of 5.23×10^{-6} for a resolvable wavelength change of 0.01 nm. To the best of our knowledge, this resolution is the highest reported to date for an all-fiber-based RI sensor without an extra-sensitive coating layer, such as an ITO [10] or surface plasmonic metal layer [11]. Table 1 compares the resolution of evanescent field fiber refractometric sensors previously published in the literature [12–18]: as demonstrated experimentally in this Letter, the resolution of the proposed STMS fiber refractometer is the highest.

In conclusion, light propagation within STMS fiber structures for RI sensing has been simulated. A maximum sensitivity of 1913 nm/RIU was achieved experimentally with an ~30 μm MMF taper waist diameter. Further optimization of the fiber sensor geometry will result in a more compact refractometric sensor device with improved performance.

P. Wang is funded by the Irish Research Council for Science, Engineering and Technology and cofunded by the Marie Curie Actions under FP7. G. Brambilla gratefully acknowledges the Royal Society (London) for his research fellowship. Q. Wu gratefully acknowledges the support of the Science Foundation Ireland under grant 07/SK/I1200.

References

1. M. Han, F. W. Guo, and Y. F. Lu, Opt. Lett. **35**, 399 (2010).
2. P. Wang, Y. Semenova, Q. Wu, G. Farrell, Y. Ti, and J. Zheng, Appl. Opt. **48**, 6044 (2009).
3. H. M. Liang, H. Miranto, N. Granqvist, J. W. Sadowski, T. Viitala, B. C. Wang, and M. Yliperttula, Sens. Actuators B Chem. **149**, 212 (2010).
4. O. Frazao, P. Caldas, J. L. Santos, P. V. S. Marques, C. Turck, D. J. Lougnot, and O. Soppera, Opt. Lett. **34**, 2474 (2009).
5. N. M. Hanumegowda, C. J. Stica, B. C. Patel, I. White, and X. Fan, Appl. Phys. Lett. **87**, 201107 (2005).
6. H. Zhu, I. M. White, J. D. Suter, M. Zourob, and X. Fan, Anal. Chem. **79**, 930 (2007).
7. F. Xu and G. Brambilla, Appl. Phys. Lett. **92**, 101126 (2008).
8. Q. Wang and G. Farrell, Opt. Lett. **31**, 317 (2006).
9. P. Wang, G. Brambilla, M. Ding, Y. Semenova, Q. Wu, and G. Farrell, J. Opt. Soc. Am. B **28**, 1180 (2011).
10. C. R. Zamarreño, M. Hernáez, I. Del Villar, I. R. Matías, and F. J. Arregui, IEEE Sens. J. **10**, 365 (2010).
11. D. Monzón-Hernández and J. Villatoro, Sens. Actuators B Chem. **115**, 227 (2006).
12. Z. Tian, S. S. Yam, and H. Loock, Opt. Lett. **33**, 1105 (2008).
13. M. Sumetsky, R. S. Windeler, Y. Dulashko, and X. Fan, Opt. Express **15**, 14376 (2007).
14. J.-L. Kou, J. Feng, Q.-J. Wang, F. Xu, and Y.-Q. Lu, Opt. Lett. **35**, 2308 (2010).
15. D. Monzón-Hernández, J. Villatoro, and D. Luna-Moreno, Sens. Actuators B Chem. **110**, 36 (2005).
16. F. Xu, P. Horak, and G. Brambilla, Opt. Express **15**, 7888 (2007).
17. F. Xu, G. Brambilla, and Y.-Q. Lu, Opt. Express **17**, 20866 (2009).
18. Q. Wu, Y. Semenova, P. Wang, and G. Farrell, Opt. Express **19**, 7937 (2011).